



Strategic use of conformational bias and structure based design to identify potent JAK3 inhibitors with improved selectivity against the JAK family and the kinome

Stephen M. Lynch^{a,*}, Javier DeVicente^a, Johannes C. Hermann^a, Saul Jaime-Figueroa^a, Sue Jin^b, Andreas Kuglstatter^c, Hongju Li^a, Allen Lovey^a, John Menke^b, Linghao Niu^b, Vaishali Patel^b, Douglas Roy^a, Michael Soth^a, Sandra Steiner^a, Parcharee Tivitmahaisoon^a, Minh Diem Vu^b, Calvin Yee^a

^aDiscovery Chemistry, Hoffmann-La Roche, pRED, Pharma Research & Early Development, 340 Kingsland Street, Nutley, NJ 07110, United States

^bInflammation Biology, Hoffmann-La Roche, pRED, Pharma Research & Early Development, 340 Kingsland Street, Nutley, NJ 07110, United States

^cDiscovery Technologies, Hoffmann-La Roche, pRED, Pharma Research & Early Development, 340 Kingsland Street, Nutley, NJ 07110, United States

ARTICLE INFO

Article history:

Received 20 November 2012

Revised 24 January 2013

Accepted 1 February 2013

Available online 13 February 2013

Keywords:

Kinase inhibitors

Janus kinase

JAK

Structure based design

Kinase selectivity

Conformational bias

ABSTRACT

Using a structure based design approach we have identified a series of indazole substituted pyrrolopyrazines, which are potent inhibitors of JAK3. Intramolecular electronic repulsion was used as a strategy to induce a strong conformational bias within the ligand. Compounds bearing this conformation participated in a favorable hydrophobic interaction with a cysteine residue in the JAK3 binding pocket, which imparted high selectivity versus the kinome and improved selectivity within the JAK family.

© 2013 Published by Elsevier Ltd.

Janus kinase 3 (JAK3) is a critical component in the pathway of all cytokines that use the common γ chain receptor for signal transduction and its deficiency has been associated with the severe combined immunodeficiency (SCID) phenotype.^{1–3} JAK3 is known to operate in concert with JAK1 in order to facilitate phosphorylation of signal transducers and activators of transcription proteins (STATs) and propagate cellular signaling.^{4,5} Recent clinical trial data for the JAK inhibitors tofacitinib (Fig. 1, **1a**) and ruxolitinib (**1b**) have offered compelling proof of concept for JAK inhibition for multiple inflammatory indications including rheumatoid arthritis (RA)^{6–10} and psoriasis,^{9,11} but also revealed side effects that could be attributable to inhibition of JAK2 and/or JAK1.^{7,8} While JAK2 and JAK1 are widely expressed, JAK3 is found predominantly in cells of hematopoietic origin.¹ Therefore selective inhibition of JAK3 may effectively suppress inflammatory signal transduction while avoiding potential side effects.

Since the JAK family of protein kinases have been clinically validated as therapeutic targets, a tremendous amount of research has been focused on identification of inhibitors derived from novel

chemotypes.^{12,13} As biological exploration of these molecules has progressed, a certain level of disagreement has emerged in the literature as to consequences of selective JAK3 inhibition.¹⁴ While one study has concluded that JAK1 inhibition is not required for efficacy in mouse models of inflammatory disease, another group has questioned whether selective inhibition of JAK3 over JAK1 will effectively modulate immunologically relevant pathways.^{15–17} Results from our in-house JAK inhibitor program, which targeted

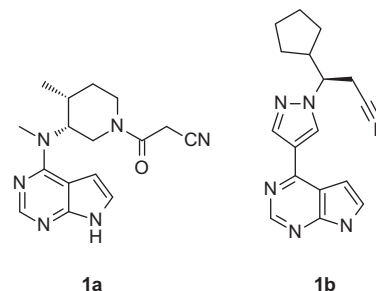
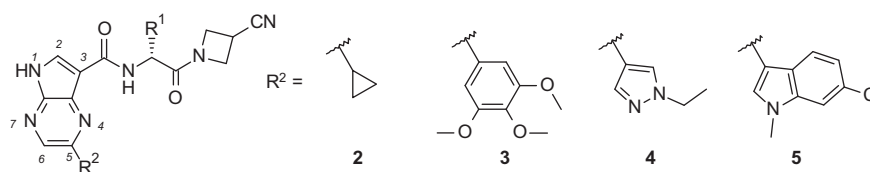


Figure 1. Structures of tofacitinib (**1a**) and ruxolitinib (**1b**).

* Corresponding author. Tel.: +1 973 235 7315; fax: +1 973 235 6263.

E-mail address: stephen.lynch@roche.com (S.M. Lynch).

Table 1Enzyme potency, selectivity and solubility data for tofacitinib, ruxolitinib and preliminary pyrrolopyrazine front pocket groups²²

Compound	R ¹	IC ₅₀ ^a (nM)			Selectivity		LYSA ^b (μg/mL)
		JAK3	JAK2	JAK1	JAK2/JAK3	JAK1/JAK3	
1a	N/A	2.2 ± 0.6	4.0 ± 0.7	1.6 ± 0.1	2	1	461
1b	N/A	10.7 ± 2.2	<0.3	0.8 ± 0.2	<1	<1	ND
2a		0.3 ± 0.1	0.8 ± 0.2	3.2 ± 1.1	3	11	33
2b		8.2 ± 1.1	37 ± 5	47 ± 16	5	6	277
3		0.4 ± 0.02	0.8 ± 0.03	7.4 ± 0.2	2	18	ND
4		5.2 ± 1.4	18 ± 4	23 ± 4	3	4	366
5		0.8 ± 0.1	3.3 ± 0.6	1.0 ± 0.2	4	1	<1

^a Mean ± SEM (standard error of the mean), $n \geq 3$ except for **3** ($n = 2$).^b LYSA = lyophilized solubility assay, ND = not determined.

inflammatory indications, suggested that compounds with improved selectivity for JAK3 over JAK1 can inhibit IL-2 signaling (which is dependent on JAK3 and JAK1) with similar potencies as less selective analogs.¹⁸

Our JAK inhibitor program relied upon a structure based approach centered around a pyrrolopyrazine hinge binding motif in which strategic substitutions at the 3-position were found to impact the observed selectivity. This exercise culminated in the identification of potent JAK family inhibitors such as the

pyrrolopyrazine bisamides **2** (Table 1) which possessed good to moderate selectivity for JAK3.¹⁸ Ligands of this type were found to impart a degree of selectivity by exploiting the unique vectors found in the bisamide sidechain to satisfy size-sensitive hydrophobic interactions in the upper and lower portions of the JAK binding pocket.

In thinking about how to further increase both the JAK family and overall pan-kinase selectivity within this promising scaffold we decided to focus on specifically targeting position 909/936,

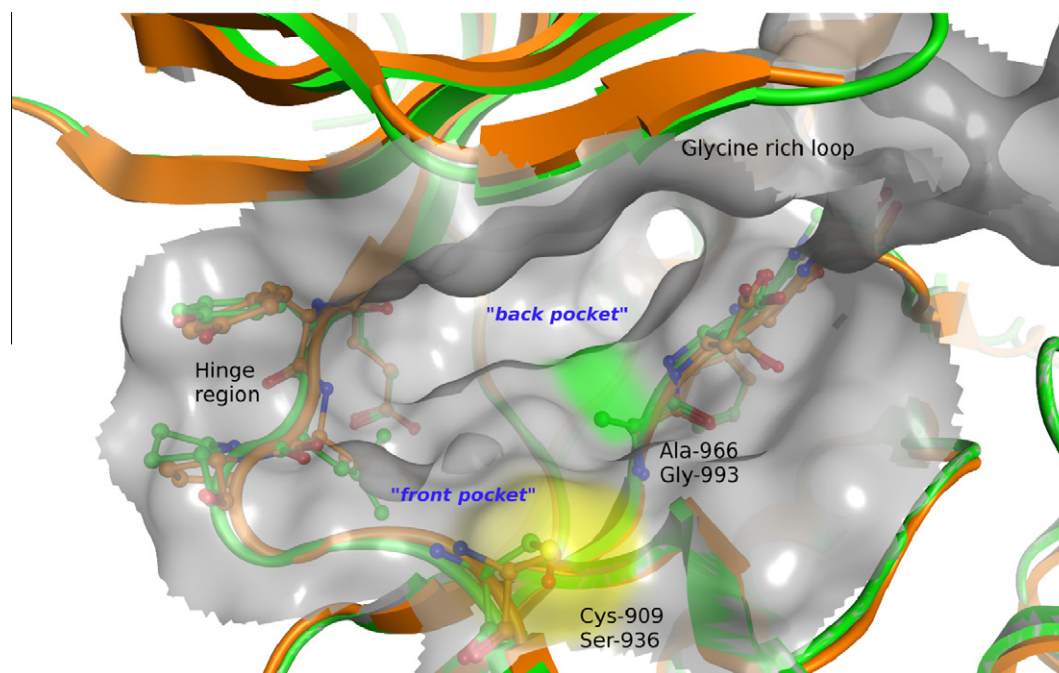


Figure 2. Superimposed crystal structures of Jak3 (carbon atoms and cartoon colored in green, PDB Code 1YVJ)¹⁹ and Jak2 (carbon atoms and cartoon colored in orange, PDB code 3JY9).²⁰ Oxygen atoms are colored in red, nitrogen atoms in blue and sulfur atoms are colored in yellow. Residue labeling corresponds to Jak2 and Jak3, respectively. All visualizations were captured with MOE.²¹

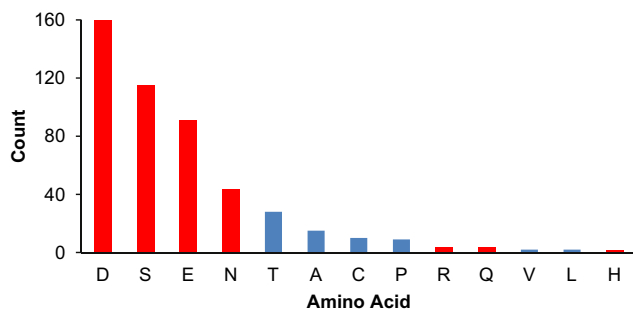


Figure 3. Prevalence of aligned amino acid residues at position 909/936 across the kinome (490 kinases). Red denotes polar, hydrophilic residues; blue denotes hydrophobic residues.

one of the two adenosine triphosphate (ATP)-binding site residues which are not conserved among JAK1, JAK2, and JAK3 (Fig. 2). While JAK3 has a cysteine in position 909, both JAK1 and JAK2 possess a more polar serine moiety at the corresponding position 936. We hypothesized that introduction of a hydrophobic substituent in this region of the binding pocket would create a favorable interaction with Cys909 but would negatively interact with Ser936 thus increasing our JAK family selectivity. Looking across the kinome, position 909/936 is typically occupied by polar residues such as aspartate, glutamate, and serine (Fig. 3). With the exception of serine, most amino acids occupying this location are more bulky than cysteine. Therefore, the combination of hydrophobic and steric interactions at this position might offer improvement in pan-kinase selectivity as well.

Our lead molecule **2a** possessed a small cyclopropyl group in the front portion of the binding pocket most close in proximity to Cys909. Our previous experience told us that analogs containing flat, aryl groups in this region such as **3** were very potent JAK3 inhibitors, but poor physicochemical properties coupled with observed JAK2 promiscuity rendered them unattractive. In an effort to identify more drug-like molecules with defined vectors for growth we became interested in small, polar heterocycles. For instance, pyrazole **4** maintained modest JAK family selectivity and offered a potential vector from N1 for interaction with cysteine. We also explored biaryl systems such as indole **5** which, although potent, did not provide the desired levels of selectivity (Table 1).

According to our molecular modeling, these compounds—in particular **5**—showed compelling potential to interact with Cys909. As a possible explanation for the observed lack of selectivity, we reasoned that free rotation around the front pocket aryl–aryl bond of conformer **5-A** could result in an equally potent conformer **5-B** (Fig. 4). This latter conformer would orient the

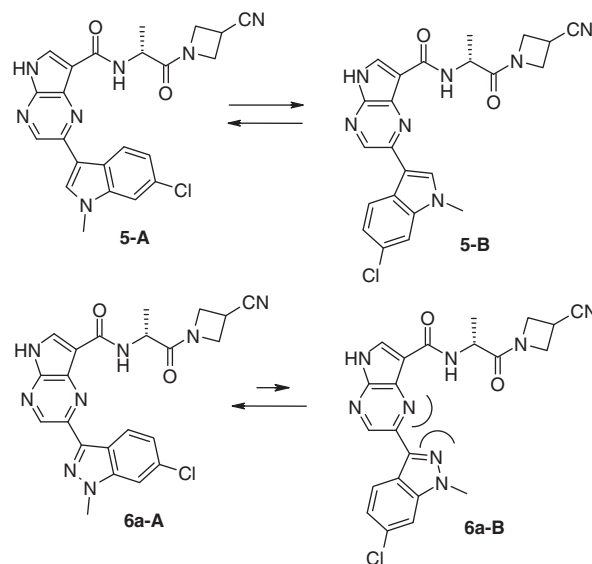


Figure 4. Conformational preferences of **5** and **6a**.

indole away from Cys909 and toward solvent where it could be accommodated equally well by all members of the JAK family.

One strategy for limiting this undesired rotation was to introduce a conformational constraint within the scaffold. Conformational constraint is a well-known medicinal chemistry strategy for preorganization of a flexible ligand into a biologically active conformation.²³ Although the constraint typically takes the form of a rigid linker, we hoped to use a strong electronic repulsion to accomplish a similar task. For instance, the N–N lone pair repulsion present in the indazole analog **6a** of indole **5** was predicted computationally to bias the molecule toward the desired conformation **A** (Fig. 4). A rotational scan of a simplified pyrazine–indazole linkage displayed a strong preference (4.7 kcal/mol) for conformer **A** in which the nitrogen lone pairs have adopted an anti-orientation (Fig. 5). When subjected to the same rotational scan, a simplified pyrazine–indole linkage showed no preference between conformations **A** and **B**.

We prepared indazole **6a** and were gratified that this compound showed good potency and a much improved JAK family selectivity profile. To probe this scaffold further, analogs bearing a variety of substitution patterns on the indazole were subsequently prepared (Table 2). The 6-Cl (**6a**) clearly showed better selectivity than the 5-Cl analog (**6b**) or the unsubstituted indazole (**6c**). Polar, planar substituents at C6 showed reasonable potency and selectivity as evidenced by compounds **6d–f**. On the other hand, substitutions

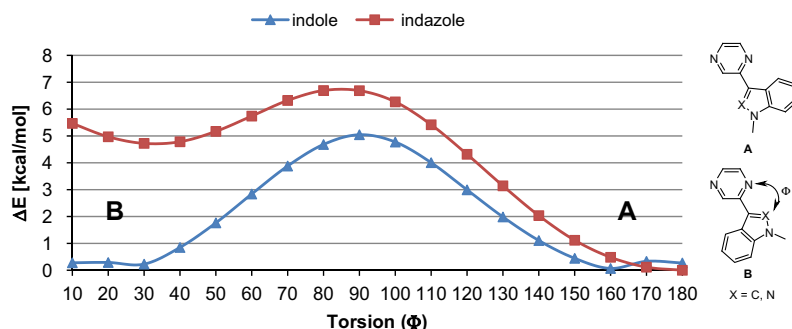
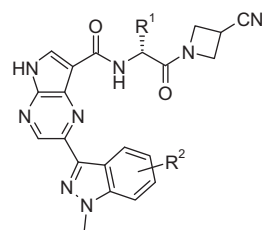


Figure 5. Rotational scan of heteroaryl-linked pyrazines. Energies are calculated at the B3LYP/6-31+G(d,p) level with Jaguar.²⁴ The torsion (ϕ) is defined as the dihedral angle between the pyrazine nitrogen and the indole/indazole 2-position. All atoms were relaxed and energy minimized freely with only ϕ fixed at each sampled angle.

Table 2Enzyme potency, selectivity and solubility data for substituted indazoles²²

Compound	R ¹	R ²	IC ₅₀ ^a (nM)			Selectivity		LYSA ^b (μg/mL)
			JAK3	JAK2	JAK1	JAK2/JAK3	JAK1/JAK3	
6a		6-Cl	1.1 ± 0.2	22 ± 0.2	31 ± 0.4	20	28	<1
6b		5-Cl	3.0 ± 0.1	28 ± 2	61 ± 3	9	20	ND
6c		H	2.9 ± 1.4	20 ± 3	22 ± 3	7	8	ND
6d		6-F	0.6 ± 0.3	12 ± 1	17 ± 1	20	28	<1
6e		6-CN	2.3 ± 1.3	38 ± 20	51 ± 41	17	22	<1
6f		6-OMe	1.8 ± 0.5	16 ± 3	38 ± 4	9	21	<1
6g		6-Cyclo-Pr	3.1 ± 0.3	15 ± 4	10 ± 2	5	3	ND
6h		6- <i>t</i> -Bu	10 ± 0.7	13 ± 1.6	12 ± 0.6	1	1	ND
6i		4-F,6-Cl	1.8 ± 0.3	56 ± 3	64 ± 2	31	36	<1
6j		6-Cl	<0.4	4.2 ± 0.6	4.6 ± 0.1	>11	>12	<1
6k		6-Cl	0.3 ± 0.06	1.1 ± 0.1	0.8 ± 0.1	4	3	ND
6l		6-Cl	0.8 ± 0.1	1.3 ± 0.1	5.5 ± 0.6	2	7	ND

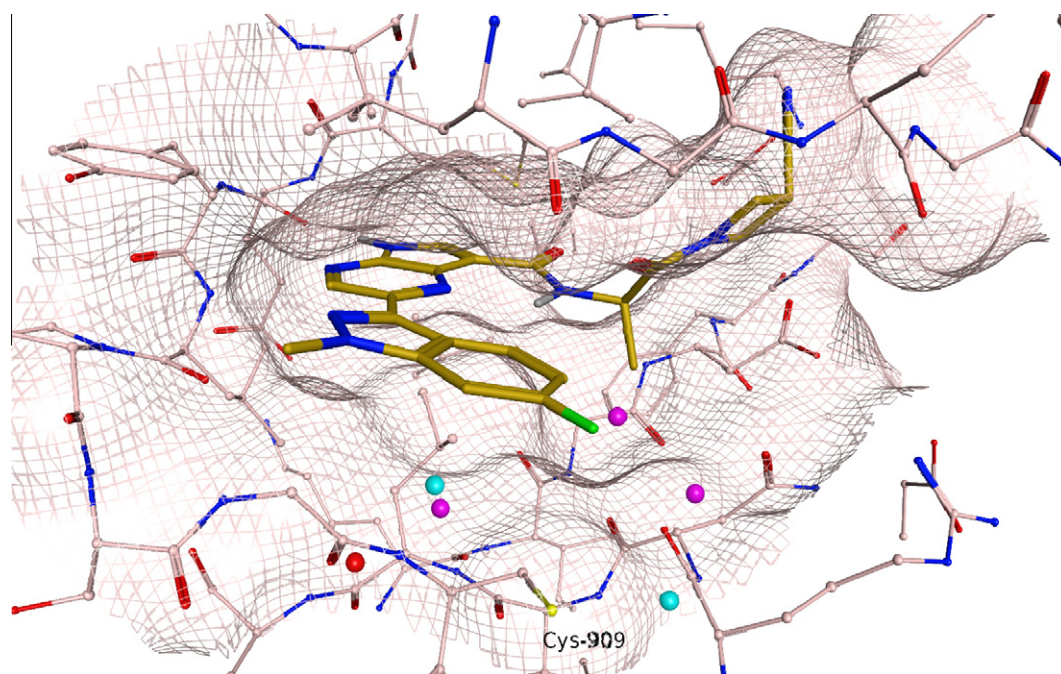
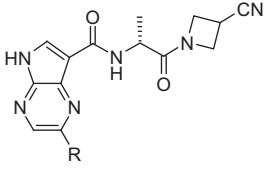
^a Mean ± SEM (standard error of the mean), $n \geq 3$ except for **6b** ($n = 2$).^b LYSA = lyophilized solubility assay, ND = not determined.

Figure 6. Crystal structure of **6d** (PDB accession number 3ZC6) in complex with Jak3 at 2.4 Å resolution.²⁶ Carbon atoms of the protein are colored in pink and ligand carbon atoms colored in gold. Nitrogen atoms are colored in blue, fluorine atoms in green, sulfur atoms in yellow and oxygen atoms including water molecules are colored in red. Displayed are also water molecule oxygen atoms close to the location of Cys-909 stemming from a superimposed Jak1 crystal structure (colored magenta, PDB code 3EYG) and a superimposed Jak2 crystal structure (colored cyan, PDB code 3FUP).²⁷

Table 3Enzyme potency, selectivity and solubility data for constrained heterobicyclic analogs²²


Compound	R	IC ₅₀ ^a (nM)			Selectivity		LYSA ^b (μg/mL)
		JAK3	JAK2	JAK1	JAK2/ JAK3	JAK1/ JAK3	
7		10.5 ± 4	83 ± 10	370 ± 38	8	35	<1
8		0.3 ± 0.07	5.9 ± 0.7	16 ± 0.6	20	53	39
9		1.0 ± 0.05	37 ± 4	73 ± 10	37	73	31
10		3.4 ± 0.9	57 ± 9	61 ± 8	17	18	ND

^a Mean ± SEM (standard error of the mean), *n* ≥ 3.^b LYSA = lyophilized solubility assay.**Table 4**

PBMC potency and selectivity data for select compounds

Compound	PBMC IC ₅₀ ^a (μM)			Selectivity	
	IL-2 ^b	GM-CSF ^c	IFN-γ ^c	GM-CSF/IL-2	IFN-γ/IL-2
1a	0.028 ± 0.001	0.184 ± 0.02	0.170 ± 0.01	7	6
1b	0.023 ± 0.003	0.026 ± 0.005	0.031 ± 0.008	1	1
2a	0.031 ± 0.003	0.19 ± 0.06	0.29 ± 0.08	6	9
3	0.10 ± 0.02	0.20 ± 0.02	0.49 ± 0.10	2	5
5	0.05 ± 0.01	0.17 ± 0.04	0.23 ± 0.07	3	5
6a	0.24 ± 0.04	>30 ^d	>30 ^d		
6d	0.15 ± 0.07	0.74 ± 0.46	1.35 ± 0.94	5	9
6f	0.18 ± 0.10	0.88 ± 0.59	2.61 ^e	5	15
6i	0.43 ± 0.06	>30 ^d	>30 ^d		
8	0.30 ± 0.20	4.23 ± 1.47	2.86 ± 0.18	14	10
9	1.29 ± 0.35	10.8 ± 2.5	12.9 ± 7.6	8	10

^a Mean ± SEM (standard error of the mean), *n* ≥ 3 except for **3**, **6d**, **6f**, **8** and **9** (*n* = 2).^b Gated on CD3 T-cells.^c Gated on CD14 monocytes.^d Low solubility was a potentially limiting factor for IC₅₀ determination.^e *n* = 1.

residing out-of-plane such as cyclopropyl (**6g**) or *tert*-butyl (**6h**) were detrimental to potency and almost completely destroyed selectivity. This suggested a limited amount of space in this region of the binding pocket. An additional fluorine at C4 (**6i**) further improved selectivity over both JAK2 and JAK1. Larger substitutions at this position were not tolerated.

We obtained a crystal structure of **6d** bound to JAK3 (Fig. 6). The structure showed the pyrrolopyrazine making the expected hinge

Table 5

Caliper profiling data for selected compounds

Kinase	5	6a	6i	6j	6k	9
ABL	79	-13	34	66	95	18
AKT1	-5	-11	-6	23	74	9
AKT2	7	6	7	-3	96	14
AMPK	88	-14	43	88	86	72
AurA	87	12	36	92	93	61
BTk	13	0	2	14	83	2
CAMK2	-53	-179	-52	-35	32	-51
CAMK4	33	-11	-24	21	47	21
CDK2	55	-4	5	23	32	36
CHK1	45	-7	-28	7	30	9
CHK2	79	1	17	58	16	80
CK1d	-3	4	9	14	75	1
c-Raf	16	20	-5	20	8	38
c-TAK1	61	-24	-11	29	67	25
DYRK1a	0	-13	12	10	16	9
Erk1	13	-5	3	24	34	5
Erk2	12	-6	3	-5	19	42
FGFR1	56	-11	13	77	80	41
FLT3	66	-7	17	28	97	24
FYN	89	-6	12	72	84	38
GSK3b	92	12	59	40	30	19
HGK	44	-17	-10	6	34	3
IGF1R	-7	-12	-30	16	-4	-7
INSR	8	-9	-4	-11	1	7
IRAK4	5	-10	-2	13	61	28
KDR	85	-18	25	54	48	39
LCK	77	-8	6	55	92	33
LYN	93	-6	3	79	74	42
MAPKAPK	1	-12	2	8	23	35
MARK1	94	-11	21	70	65	65
MET	2	-15	-3	12	99	-1
MSK1	6	4	9	12	92	9
MST2	83	11	50	83	69	60
p38a	-4	-7	4	-6	27	-3
p70S6K	-14	-12	-33	-12	32	-42
PAK2	29	-7	7	-29	26	10
PIM2	-18	-15	-64	3	91	-9
PKA	56	-5	-2	25	24	13
PKCb	-5	-5	1	13	46	9
PKCz	13	7	4	14	27	11
PKD2	3	-2	1	16	80	6
PKGa	4	0	4	8	11	0
PRAK	1	-4	-2	0	22	-12
ROCK2	94	4	36	50	30	61
RSK1	73	8	17	40	72	31
SGK1	17	-17	14	20	99	21
SRC	91	-3	12	72	70	35
SYK	95	25	60	89	96	40

Values represent percent inhibition at 10 μM concentration (green <50%; red >95%).

binding interaction. The bisamide sidechain also adopted the anticipated conformation with the methyl group shallowly filling the back lower region of the pocket and the cyanoazetidine angled upward under the glycine rich loop. The indazole occupied the front region of the pocket and displayed an approximate 15° tilt downward to rest over top of Cys909 and make a favorable hydrophobic contact. Substituents at the indazole 6-position appear to be in closest proximity to residues 909/936 and would be expected to displace conserved waters associated with the polar network surrounding Ser936 in JAK2 and JAK1.²⁵ While displacement of these waters would require a larger energetic penalty for JAK2 and JAK1, the hydrophobic cysteine interactions present in JAK3 could compensate for the water loss, thus contributing to the observed selectivity. Excessive steric bulk in this region presumably interferes

with optimal cysteine hydrophobic contact causing a loss in JAK3 potency. The 4-fluorine present in analog **6i** likely favors a non-planar orientation of the indazole sidechain relative to the pyrrolopyrazine core, thus enforcing a downward tilt of the indazole towards Cys909.

We knew from our previous investigations that placement of large, hydrophobic substituents in the back, lower binding pocket generally increased both potency and selectivity toward JAK3 (compare **2a** and **2b**). To examine possible synergy between the front pocket indazole and the lower pocket group, analogs **6j–i** bearing progressively larger R¹ substituents were prepared. Although these three compounds were exceedingly potent toward JAK3, a dramatic decrease in JAK family selectivity was observed suggesting an intricate interplay between the indazole in the front pocket and the alkyl lower pocket group. Steric clash between the indazole and bulky lower pocket groups may alter the torsion of the indazole–pyrrolopyrazine bond, tilting the indazole away from position 909/936. This new conformation might no longer disfavor JAK2 and JAK1 and account for the observed increase in potency toward both of these enzymes. Presumably the lower pocket methyl group is optimal for both shallow space filling and allowing an ideal indazole torsion.

In light of the successful results obtained with the indazole front pocket group we decided to explore several additional heterocycles at this position (Table 3). In principal, any 5,6-heterobicyclic system in the front pocket could impart a similar conformational bias, however diversified distribution of electronics in the region of Cys909/Ser909 might be a factor in the overall JAK family selectivity. Although less potent, N-1 linked indazoles such as **7** were determined to be JAK3 selective inhibitors. Of greater interest were the imidazo[1,5]pyridines such as **8** and **9**. The difluoro analog **9** was particularly selective within this series. Of note was the imidazo[1,2]pyridine **10** which was also observed to have reasonable potency and good JAK3 selectivity even though it lacked the key nitrogen ortho to the biaryl linkage. Rotational scan of this scaffold (as described in Fig. 5) reinforced this result by predicting a >4 kcal/mol energy difference favoring the desired conformation. One benefit of the imidazo[1,5] pyridines **8** and **9** was their

improved solubility compared to the indazoles **6** and **7** as measured by the LYSA (lyophilized solubility) assay.

In order to assess the JAK family selectivity of these compounds in a more biologically relevant system, select examples were tested in a cellular functional assay. This assay measured inhibition of phosphorylation of downstream STAT proteins in peripheral blood mononuclear cells (PBMCs) upon treatment with varying stimuli. Thus, stimulation with IL-2, GM-CSF, or IFN- γ induces JAK3/1, JAK2, or JAK2/1 mediated phosphorylation of STAT5a, STAT5a, or STAT1, respectively (Table 4). Initial lead compound **2a** showed good potency in these assays with preference observed for inhibition of IL-2 signaling versus GM-CSF and IFN- γ signaling. Similar cellular potencies and selectivities were observed for tofacitinib **1a**, and slightly lower cellular selectivities for trimethoxyphenyl analog **3** and indole analog **5**. In contrast, ruxolitinib **1b**, while potent in our cellular assays, showed no cellular selectivities. Ruxolitinib **1b** is a JAK1/2 inhibitor with a relatively large selectivity window (>10-fold) versus JAK3 in our enzyme assays, while **1a**, **2a**, **3**, and **5** are all pan-JAK or modestly JAK3-selective inhibitors. We therefore conclude that more potent JAK3 inhibition relative to JAK1 and/or JAK2 inhibition can improve selectivity for inhibition of our IL-2 cellular assay versus our GM-CSF and IFN- γ assays.

The effects of further improvements in JAK3 versus JAK2 and JAK1 enzyme selectivities upon cellular selectivities are subtle and equivocal. While the results for indazoles **6a** and **6i** suggest a greatly improved cellular selectivity in our assays, the more modest cellular selectivities observed for other compounds with similar or better JAK3 enzyme selectivities temper that initial conclusion. The indazoles in general exhibited poor solubilities (Table 2), and this issue may have been a limiting factor for accurate IC₅₀ determination for **6a** and **6i** in the GM-CSF and IFN- γ assays. However, we were able to determine definitive IC₅₀ curves for all other examples in Table 4 and will focus our discussion on those compounds.

All of the JAK3 versus JAK2 and JAK1 enzyme selective examples show cellular selectivities inhibiting IL-2 versus GM-CSF and IFN- γ signaling, and the overall trend appears to be that improving selectivity for inhibition of JAK3 versus JAK2 and JAK1 results in

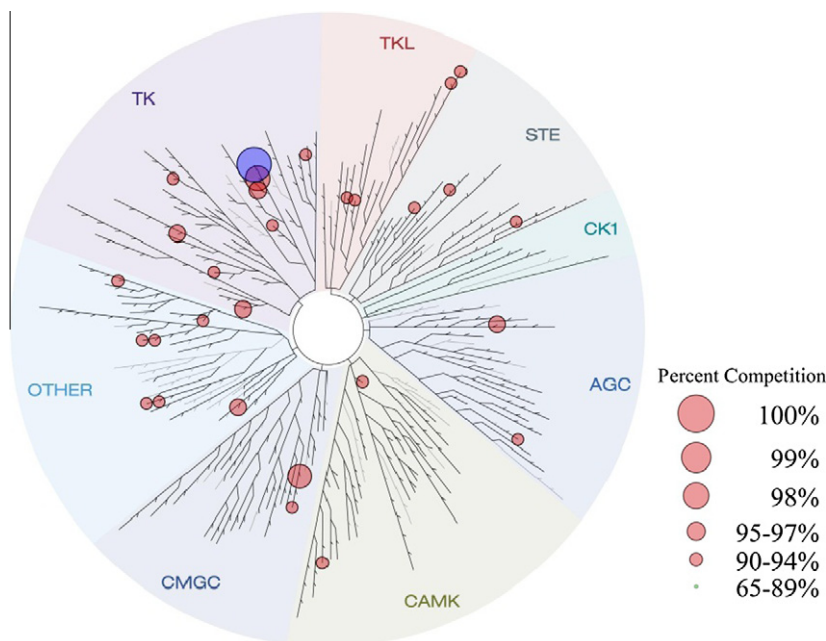


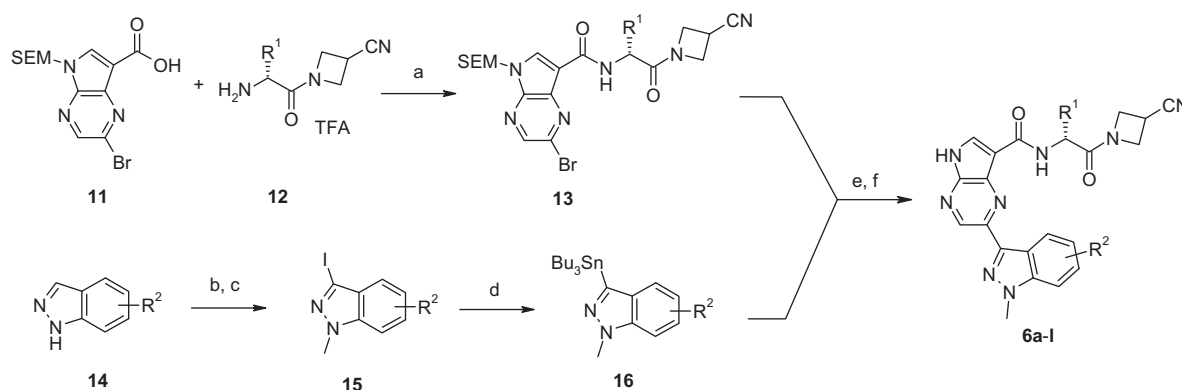
Figure 7. Kinomescan dendrogram of **6a** versus 442 kinases at 10 μ M. JAK3 is shaded in blue.

an improved cellular selectivity for inhibiting IL-2 versus GM-CSF and IFN- γ signaling. For example, the most JAK3-selective examples, compounds **8** and **9**, demonstrate approximately 10-fold improved cellular selectivities compared to the least JAK3-selective example, the JAK1/2 inhibitor ruxolitinib **1b**. However, it is difficult to define an exact relationship between enzyme and cellular selectivities; for example, the cellular selectivities observed for indazole **6d** are similar to those seen for the less enzyme-selective examples **2a** and tofacitinib **1a**. This continuing uncertainty underscores the complexity of JAK/STAT signaling.

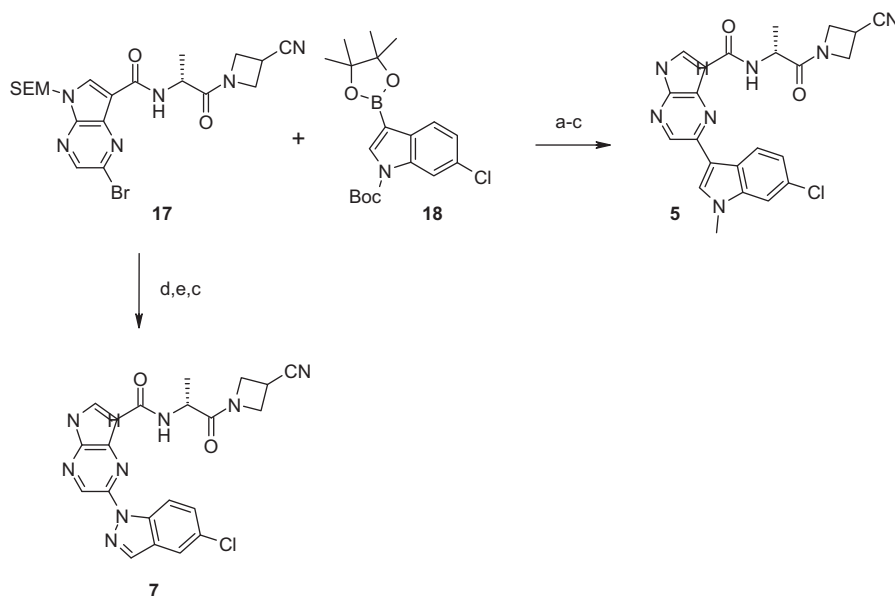
To evaluate kinase selectivity, we profiled compounds by Caliper screening against a 48 kinase panel. Caliper profiling measures percent inhibition of phosphorylation of a peptide substrate.²⁸ The data in Table 5 is represented by a heat map, assigning <50% inhibition as completely green and >95% inhibition as completely red. The Caliper data clearly indicate that indazoles **6a** and **6i** demonstrated greater pan-kinase selectivity than indole **5**. Indazoles **6j** and **6k**, which possessed larger lower pocket functionality lost selectivity versus the kinase. This result highlights the significance of interplay between the front pocket and lower

pocket alkyl substituent not only for JAK family selectivity but for pan-kinase selectivity as well. Imidazo[1,5]pyridine **9** also showed a reasonable selectivity profile against this panel of kinases, which confirms the observed trend with a more soluble analog. For more comprehensive profiling **6a** was assayed using the Kinomscan platform.²⁹ Data generated at 10 μ M showed that this compound was quite selective against a panel of 442 wild-type kinases, displacing >90% of ligand in only 29 cases (Fig. 7). K_d values against the kinase domains of JAK3 (1.4 nM), JAK2 (11 nM), JAK1 (73 nM), and Tyk2 (350 nM) were also determined for **6a**. Although these K_d s are not exactly correlated with our in-house results, they overall confirm our observed JAK family selectivities and also show that this ligand discriminates against Tyk2, the final member of the JAK family.

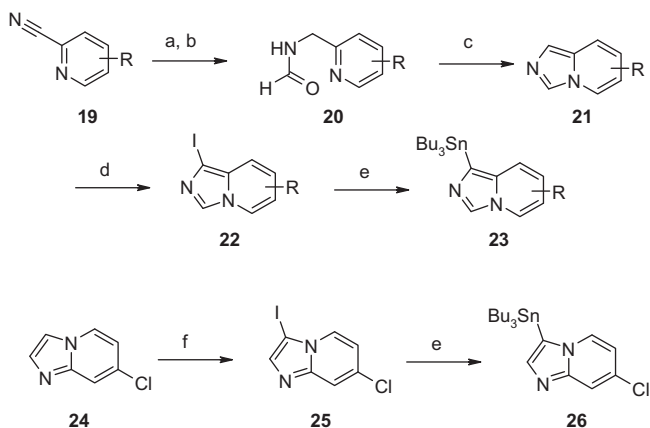
The indazole substituted pyrrolopyrazines described were synthesized using the convergent approach outlined in Scheme 1. Amine salts **12** were prepared by coupling of the appropriate Boc-protected amino acid with 4-cyanoazetidine followed by Boc deprotection. The SEM protected pyrrolopyrazine acid **11** was then coupled to the amine salt **12** to provide bromine containing



Scheme 1. Synthesis of indazoles **6a-l**. Reagents and conditions: (a) HATU, *i*-Pr₂NEt, DMF, rt; (b) I₂, KOH, DMF, rt; (c) KOT-Bu, MeI, 0 °C to rt; (d) *i*-PrMgCl, THF, –10 °C then Bu₃SnCl, –10 °C to rt; (e) Pd(PPh₃)₄, CuI, DMF, 85 °C, 2 h; (f) TFA, CH₂Cl₂ then ethylenediamine, CH₂Cl₂.



Scheme 2. Synthesis of indole **5** and indazole **7**. Reagents and conditions: (a) Pd(PPh₃)₄, Na₂CO₃, DME, H₂O, 90 °C, overnight, 52%; (b) NaH, DMF, 0 °C then MeI, 61%; (c) TFA, CH₂Cl₂ then ethylenediamine, CH₂Cl₂, 58–63%; (d) CuI, NaI, *trans*-*N,N'*-dimethylcyclohexane-1,2-diamine, 1,4-dioxane, 110 °C, 48 h; (e) CuI, K₃PO₄, *trans*-*N,N'*-dimethylcyclohexane-1,2-diamine, 5-chloro-1*H*-indazole, toluene, 110 °C, 24 h, 58% (2 steps).



Scheme 3. Synthesis of imidazo[1,5]pyridinyl- and imidazo[1,2]pyridinyl stannanes. Reagents and conditions: (a) H_2 (45 psi), Pd/C, concd HCl, EtOH, 3.5 h; (b) HCO_2H , 110 °C, overnight; (c) $POCl_3$, toluene, 110 °C, 24–29% (3 steps); (d) I_2 , $NaHCO_3$, EtOH/ H_2O , rt, 27–38%; (e) i -PrMgCl, THF, –10 °C then Bu_3SnCl , –10 °C to rt, 83–90%; (f) n -BuLi, THF, –50 °C then N -iodosuccinimide, –50 to 0 °C.

bisamide **13**. Substituted indazoles **14** were iodinated and selectively methylated at N-1 under basic conditions (N1:N2 ratio ~3:1). Grignard exchange at low temperature followed by quenching with tributyltin chloride provided the stannanes **16**. Stille coupling and a two-stage SEM deprotection afforded the target molecules **6a–l**.

Indole **5** was prepared as described in Scheme 2. Suzuki coupling of bromide **17** and indole boronic ester **18** proceeded with concomitant loss of the Boc protecting group. Selective N-methylation of the indole nitrogen followed by SEM deprotection afforded **5**. The N1-linked indazole derivative **7** was prepared from bromide **17** using the copper catalyzed halide exchange/N-arylation sequence developed by Buchwald.³⁰

Imidazo[1,5]pyridines were synthesized according to the route illustrated in Scheme 3. Hydrogenation of 2-cyanopyridines **19** followed by formylation in refluxing formic acid afforded the formates **20**. Treatment with phosphorous oxychloride followed by heating induced cyclization to the appropriately substituted imidazo[1,5]pyridines **21** in moderate yield for the three step sequence. Iodination followed by Grignard exchange and quenching with tributyltin chloride provided the stannanes **23** required for synthesis of **8** and **9** through Stille coupling and deprotection as described above. Likewise, commercially available 7-chloroimidazo[1,2]pyridine **24** was converted to **10** via the stannane **26**.

In conclusion, using a structure based approach, we have discovered a potent series of indazole-substituted pyrrolopyrazine JAK3 inhibitors which show excellent pan-kinase and improved JAK family selectivity at an enzyme level. We attribute our observed selectivity to hydrophobic interactions with a cysteine residue rare to the JAK3 binding pocket. Electronic repulsion was used as a tool to induce conformational bias within the ligand which favored the desired hydrophobic interaction and imparted the observed improvement in kinase selectivity. This strategy was found to be general in nature and was subsequently applied to additional preclinical kinase inhibitor discovery programs.

Acknowledgment

The authors wish to thank David Goldstein for his support of this work.

References and notes

- O'Shea, J. J.; Pesu, M.; Borie, D. C.; Changelian, P. S. *Nat. Rev. Drug Disc.* **2004**, *3*, 555.
- Macchi, P.; Villa, A.; Giliani, S.; Sacco, M. G.; Frattini, A.; Porta, F.; Ugazio, A. G.; Johnston, J. A.; Candotti, F.; O'Shea, J. J.; Vezzoni, P.; Notarangelo, L. D. *Nature* **1995**, *377*, 65.
- Russell, S. M.; Tayebi, N.; Nakajima, H.; Riedy, M. C.; Roberts, J. L.; Aman, M. J.; Migone, T. S.; Noguchi, M.; Markert, M. L.; Buckley, R. H.; O'Shea, J. J.; Leonard, W. J. *Science* **1995**, *270*, 797.
- Ghoreschi, K.; Laurence, A.; O'Shea, J. J. *Immunol. Rev.* **2009**, *228*, 273.
- Pesu, M.; Laurence, A.; Kishore, N.; Zwillich, S. H.; Chan, G.; O'Shea, J. J. *Immunol. Rev.* **2008**, *223*, 132.
- Flanagan, M. E.; Blumenkopf, T. A.; Brissette, W. H.; Brown, M. F.; Casavant, J. M.; Chang, S.-P.; Doty, J. L.; Elliott, E. A.; Fisher, M. B.; Hines, M.; Kent, C.; Kudlacz, E. M.; Lillie, B. M.; Magnuson, K. S.; McCurdy, S. P.; Munchhof, M. J.; Perry, B. D.; Sawyer, P. S.; Strelevitz, T. J.; Subramanyam, C.; Sun, J.; Whipple, D. A.; Changelian, P. S. *J. Med. Chem.* **2010**, *53*, 8468.
- Riese, R. J.; Krishnaswami, S.; Kremer, J. *Best Pract. Res. Clin. Rheumatol.* **2010**, *24*, 513.
- Kremer, J. M.; Bloom, B. J.; Breedveld, F. C.; Coombs, J. H.; Fletcher, M. P.; Gruben, D.; Krishnaswami, S.; Burgos-Vargas, R.; Wilkinson, B.; Zerbini, C. A.; Zwillich, S. H. *Arthritis Rheum.* **2009**, *60*, 1895.
- West, K. *Curr. Opin. Invest. Drugs* **2009**, *10*, 491.
- Incyte's JAK inhibitor demonstrates rapid and marked clinical improvement in rheumatoid arthritis patients. Incyte Corporation press release, October 26, 2008. <http://investor.incyte.com/phoenix.zhtml?c=69764&p=irol-newsArticle&ID=1217246&highlight> (accessed January 23, 2013).
- Punwani, N.; Scherle, P.; Flores, R.; Shi, J.; Liang, J.; Yeleswararam, S.; Levy, R.; Williams, W.; Gottlieb, A. *J. Am. Acad. Dermatol.* **2012**, *67*, 658.
- Wilson, L. J. *Expert Opin. Ther. Pat.* **2010**, *20*, 609.
- Wroblewski, S. T.; Pitts, W. J. *Ann. Rep. Med. Chem.* **2009**, *44*, 247.
- Ghoreschi, K.; Laurence, A.; O'Shea, J. J. *Nat. Immunol.* **2009**, *10*, 356.
- Lin, T. H.; Hegen, M.; Quadros, E.; Nickerson-Nutter, C. L.; Appell, K. C.; Cole, A. G.; Shao, Y.; Tam, S.; Ohlmeyer, M.; Wang, B.; Goodwin, D. G.; Kimble, E. F.; Quintero, J.; Gao, M.; Symanowicz, P.; Wrocklage, C.; Lussier, J.; Schelling, S. H.; Hewet, A. G.; Xuan, D.; Krykbaev, R.; Togias, J.; Xu, X.; Harrison, R.; Mansour, T.; Collins, M.; Clark, J. D.; Webb, M. L.; Seidl, K. J. *Arthritis Rheum.* **2010**, *62*(8), 2283.
- Thoma, G.; Nuninger, F.; Falchetto, R.; Hermes, E.; Tavares, G. A.; Vangrevelinghe, E.; Zerwes, H.-G. *J. Med. Chem.* **2011**, *54*, 284.
- Haan, C.; Rolvering, C.; Raulf, F.; Kapp, M.; Druckes, P.; Thoma, G.; Behrmann, I.; Zerwes, H.-G. *Chem. Biol.* **2011**, *18*, 314.
- Soth, M.; Hermann, J.; Yee, C.; Alam, M.; Barnett, J. W.; Berry, P.; Browner, M. F.; Harris, S.; Hu, D.-Q.; Jaime-Figueroa, S.; Jahangir, A.; Jin, S.; Frank, K.; Frauchiger, S.; Hamilton, S.; He, Y.; Hendricks, T.; Hilgenkamp, R.; Ho, H.; Kutach, A. K.; Hekmat-Nejad, M.; Henningsen, R.; Hoffman, A.; Hsu, J.; Itano, A.; Kuglstat, A.; Liao, C.; Lynch, S.; Menke, J.; Niu, L.; Patel, V.; Railkar, A.; Roy, D.; Shao, A.; Shaw, D.; Steiner, S.; Sun, Y.; Tan, S.-L.; Wang, S.; Vu, M. D. *J. Med. Chem.* **2013**, *56*, 345.
- Boggon, T. J.; Li, Y.; Manley, P. W.; Eck, M. J. *Blood* **2005**, *106*, 996.
- Wang, T.; Duffy, J. P.; Wang, J.; Halas, S.; Salituro, F. G.; Pierce, A. C.; Zuccola, H. J.; Black, J. R.; Hogan, J. K.; Jenson, S.; Shlyakter, D.; Mahajan, S.; Gu, Y.; Hoock, T.; Wood, M.; Furey, B. F.; Frantz, J. D.; Dauffenbach, L. M.; Germann, U. A.; Fan, B.; Namchuk, M.; Bennani, Y. L.; Ledebner, M. W. *J. Med. Chem.* **2009**, *52*, 7938.
- Molecular Operating Environment (MOE)*, 2011.10; Chemical Computing Group Inc., 1010 Sherbrooke St. West, Suite #910, Montreal, QC, Canada H3A 2R7, 2011.
- Enzyme assay measured inhibition of phosphorylation of a biotinylated synthetic peptide catalyzed by JAK1, JAK2 or JAK3. All enzymes reactions were run at adenosine triphosphate (ATP) concentrations of 1.5 μ M. K_m 's of these enzymes for ATP were determined to be 1.5 μ M (JAK3), 6 μ M (JAK2), and 20 μ M (JAK1).
- Martin, S. F. *Pure Appl. Chem.* **2007**, *79*, 193.
- Jaguar, version 7.8, Schrödinger, LLC, New York, NY, 2011.
- Michel, J.; Tirado-Rives, J.; Jorgensen, W. L. *J. Am. Chem. Soc.* **2009**, *131*, 15403.
- X-ray crystal structure determined by Proteros Biostructures GmbH (Martinsried, Germany).
- Williams, N. K.; Bamert, R. S.; Patel, O.; Wang, C.; Walden, P. M.; Wilks, A. F.; Fantino, E.; Rossjohn, J.; Lucet, I. S. *J. Mol. Biol.* **2009**, *387*, 219.
- Dunne, J.; Reardon, H.; Trinh, V.; Li, E.; Farinas, J. *Assay Drug Dev. Technol.* **2004**, *2*, 121.
- Fabian, M. A. B.; William, H.; Treiber, D. K.; Atteridge, C. E.; Azimioara, M. D.; Benedetti, M. G.; Carter, T. A.; Cicci, P.; Edeen, P. T.; Floyd, M.; Ford, J. M.; Galvin, M.; Gerlach, J.; Grotzfeld, R. M.; Herrgard, S.; Insko, D. E.; Insko, M. A.; Lai, A. G.; Lelias, J.; Mehta, S. A.; Milanov, Z. V.; Velasco, A. M.; Wodicka, L. M.; Patel, H. K.; Zarrinkar, P. P.; Lockhart, D. J. *Nat. Biotechnol.* **2005**, *23*, 329.
- Antilla, J. C.; Baskin, J. M.; Barder, T. E.; Buchwald, S. L. *J. Org. Chem.* **2004**, *69*, 5578.